Characterization and antioxidant activities of intracellular polysaccharides from Agaricus bitorquis (QuéL.) Sacc. Chaidam ZJU-CDMA-12

Hui Kuang, Yingchun Jiao, Wei Wang, Fengju Wang, Qihe Chen

PII: S0141-8130(19)35142-6

DOI: https://doi.org/10.1016/j.ijbiomac.2019.11.142

Reference: BIOMAC 13923

To appear in: *International Journal of Biological Macromolecules*

Received date: 5 July 2019

Revised date: 16 November 2019

Accepted date: 18 November 2019

Please cite this article as: H. Kuang, Y. Jiao, W. Wang, et al., Characterization and antioxidant activities of intracellular polysaccharides from Agaricus bitorquis (QuéL.) Sacc. Chaidam ZJU-CDMA-12, *International Journal of Biological Macromolecules*(2018), https://doi.org/10.1016/j.ijbiomac.2019.11.142

Characterization and antioxidant activities of intracellular polysaccharides from *Agaricus bitorquis* (QuéL.) Sacc. Chaidam ZJU-CDMA-12

Hui Kuang [1], Yingchun Jiao [2], Wei Wang [3], Fengju Wang [1], Qihe Chen [1,*]

[1] *Department of Food Science and Nutrition, Zhejiang University, Hangzhou 310058, China*

[2] *Agriculture and Animal Husbandry College, Qinghai University, Xining 810016, China*

[3] *Institute of Quality and Standard for Agriculture Products, Zhejiang Academy of Agriculture Sciences, Hangzhou 310021, China*

Email addresses of all authors:

Hui Kuang: 11813032@zju.edu.cn

Yingchun Jiao: jiaoyingchun@qhu.edu.cn

Wei Wang: 13738132996@126.com

Fengju Wang: 3150100482@zju.edu.cn

Corresponding author:

Qihe Chen

Yuhangtang Rd. 866

Department of Food Science and Nutrition

Zhejiang University

Hangzhou 310058

P.R.China

Tel: +86-571-86984316

E-mail: chenqh@zju.edu.cn

Abstract

The antioxidant activities of polysaccharides from the fruiting body (PFB), extracellular polysaccharides (EPS) and intracellular polysaccharides (IPS) from *Agaricus bitorquis* (QuéL.) *Sacc.* Chaidam ZJU-CDMA-12 in *vitro* were compared. IPS showed stronger antioxidant activities than PFB and EPS in *vitro*. Further purification and structure analyses indicated that IPS mainly consisted of three fractions (IPS-I, IPS-II and IPS-III). FT-IR and NMR data indicated that IPS was mainly composed of (1→6)-linked α-D-glucose. There are significant differences of antioxidant activities among IPS-I, IPS-II and IPS-III fractions in *vitro*, and IPS-III showed stronger antioxidant activity than IPS-I and IPS-II. IPS-III also possesses a potent antioxidant ability inside HepG2 cells, and it could protect HepG2 cells from H_2O_2-induced cytotoxicity by scavenging overproduced cellular ROS and inhibiting SOD, CAT and GSH depletion to weaken lipid peroxidation. These findings suggested that IPS-III could be a novel antioxidant and that it could afford protection against H_2O_2-induced cytotoxicity and oxidative stress.

Keywords: Antioxidant activities; polysaccharides; *Agaricus bitorquis* (QuéL.) *Sacc.* Chaidam

1. Introduction

Reactive oxygen species (ROS) and free radicals are produced with the normal metabolism of oxygen in human body, but overproduced ROS and free radicals caused by oxidative stress are proved to be associated with many acute and chronic pathologies, such as cancer, cardiovascular diseases, diabetes, hypertension, atherosclerosis, inflammation, ageing and liver injury [1]. Natural effective antioxidants such as polyphenols, vitamin C, flavonoids, and polysaccharides have proved to show good effects on alleviating oxidative stress and preventing the physiological damage on organism. Recently, researchers have taken more focus on finding natural and effective antioxidants to replace the synthetic antioxidants such as butylated hydroxytoluene (BHT) and butylated hydroxyanisole (BHA) because of its potential damages to human bodies.

Agaricus bitorquis (Quél.) Sacc. Chaidam (ABSC) is a specific wild macro fungus in Qaidam Basin (Qinghai province, China), and its fruiting bodies are known as a popular edible and medicinal food resource for its plentiful nutrition and bioactive compounds, such as polysaccharides, glycopeptide complexes, and phenolic acids. Polysaccharides are the most widely studied mushroom-derived bioactive substances for their various biological functions. Polysaccharides extracted from the fruit bodies and mycelium of fungus are proved to exhibit different pharmacological activities, such as anti-tumoral activities, immunostimulatory activity, anti-hyperlipidemia activity, anti-inflammatory activity, and antioxidant activity [2-4]. Especially, more investigations have proved that polysaccharides from medicinal fungi such as *Cordyceps sinensis*, *Agaricus bisporus*, *Dictyophora indusiata* had significant antioxidant activity on 1-diphenyl-2-picrylhydrazyl (DPPH), superoxide anion and hydroxyls radicals[5]. For example, Jing et al. (2018) reported that exopolysaccharides from the

medicinal mushroom *Ganoderma lingzhi* (GLEPS) with higher carbohydrate and uronic acid contents exhibited strong antioxidant activities in vitro via scavenging radicals, reducing power, and chelating of transition metal catalysis [6]. Zhang et al. (2016) founded that intracellular polysaccharides (IPS-1 and IPS-2) from *Pleurotus eryngii* SI-04 mycelia showed antioxidant activities and that especially IPS-2 showed obvious scavenging capacity to superoxide anion, DPPH and hydroxyl radicals [7].

Though there were many relevant reports about properties and biological activities of polysaccharide extracts from edible and medicinal fungi, few studies has been carried out on the properties and biological activities of polysaccharides from the fruiting bodies (PFB), extracellular polysaccharide (EPS) and intracellular polysaccharide (IPS) of ABSC. In previous work, we discovered that PFB, EPS and IPS from ABSC possessed potent anti-hypoxic activity [8, 9], which inspired us to explore other potential functional and medicinal value of ABSC. In this study, the antioxidant activities of ABSC polysaccharides including PFB, IPS and EPS in *vitro* were investigated, and the primary structural characterization of IPS was also conducted to have a better understanding of its structures. Then the protective effects of IPS-III (a fractions of IPS that showed the strongest antioxidant activity) on oxidative damaged HepG2 cells were also conducted to further evaluate its anti-antioxidant activities. It is noteworthy to investigate the bioactivity of such polysaccharides from ABSC in order to lay the foundation for further development of this mushroom in nutritional and therapeutic applications.

2. Materials and methods

2.1. Materials and regents

The fruiting bodies of *Agaricus bitorquis* (QuéL.) *Sacc*. Chaidam mushroom collected

from Qinghai Province, China, were provided by the Wild Plants Resources Institute of Qinghai Academy of Agriculture and Forestry Science (Xining, China) and it was identified by Professor Y.C. Jiao (Qinghai University, Xining, China). They were freeze-dried after removing any residual compost and were cut into pieces. Then, lyophilized mushrooms were grinded into powder. The inclining strain ZJU-CDMA-12 of ABSC was preserved in China Center for Type Culture Collection (CCTCC M 2018250). HepG2 cells were purchased from the Cell Bank of Type Culture Collection of the Chinese Academy of Sciences (Shanghai, China) and grown in Dulbecco's modified Eagle's medium (DMEM) (CORNING Co. Ltd, USA) which contained 10% fetal bovine serum (GIBCO/Invitrogen, Carlsbad, USA) and 1% antibiotic-antimycotic solution (GIBCO/Life Technologies, Carlsbad, USA). Cells were cultured at 37 ^{o}C in a humidified atmosphere with 5% CO_2. Kits for determination of total superoxide dismutase (T-SOD), glutathione peroxidase (GSH-Px), lipid peroxidation (MDA) and catalase (CAT) were acquired from Beyotime Institute of Biotechnology (Shanghai, China). All other chemicals used were of analytical grades.

2.2. Preparation of crude polysaccharide extracts

PFB was extracted twice from the fruiting bodies of ABSC with hot water in a 1: 30 (w/v) ratio for 3 h, and then four volumes of ethanol were added and precipitated overnight at 4 ^{o}C as described previously [8]. Then it was processed by concentration, precipitation, centrifugation and lyophilization to obtain crude PFB as reported previously [8]. In the preparation of EPS, the fermentation medium (maltobiose 20%, glucose 10%, peptone 5%, KH_2PO_4 1.0%, $MgSO_47H_2O$ 0.5%, vitamin B1 0.5%, pH 5.0, w/v) was prepared, and then incubated for 14 d at 23 ^{o}C with shaking at 130±5 rpm. Similar to PFB, the fermentation broth and cultured mycelia were processed by con-

centration, precipitation, centrifugation and lyophilization to obtain crude EPS and IPS as reported before [8].

2.3. Purification of polysaccharides

All the treatments were followed as described previously [8]. After being destained with activated carbon, PFB, EPS and IPS (200 mg each) were dissolved in 10 mL of distilled water, respectively, then the proteins in these polysaccharides were removed by using the Sevage reagent (*V* polysaccharide extracts: *V* n-butanol: *V* chloroform = 3:1:5). The supernatant was purified after centrifugation on an anion exchange column (2.5 cm × 70 cm) with DEAE-52 cellulose. Eluting process was performed with distilled water at a flow rate of 1 mL/min. The eluates were collected and carbohydrates were monitored by the phenol sulfuric acid method [10]. The collected fractions were pooled, desalted and further purified on a Sephadex G-200 column eluting with distilled water at 0.5 mL/min. The major polysaccharide fractions were pooled and lyophilized.

2.4. In vitro antioxidant activity evaluation

2.4.1. DPPH radical scavenging activity

The DPPH radical scavenging assay was used to test the antioxidant activity of PFB, EPS and IPS [11]. The Trolox (0.05–1.5 mM) were used as the standard of reference. The EC_{50} value is calculated which leads to the elimination of 50% DPPH radicals. The DPPH radical scavenging capacity (%) of the investigated samples were calculated by the following equation:

$$DPPH\ radicals\ cavening\ activity(\%) = \left(1 - \frac{A1 - A2}{A0}\right) \times 100$$

Where *A*0 was the absorbance of the blank group (distilled water + DPPH), *A*1 was the absorbance of the sample reaction (sample + DPPH), and *A*2 was the back ground absorbance of the sample (sample + 75% ethanol aqueous solution).

2.4.2. ABTS radical scavenging activity

ABTS radical scavenging activity was measured by the method described previously by Kozics et al. [12] with some modifications. The ABTS solution was diluted with PBS (pH 7.4) to give an absorbance of 0.70 ± 0.05 at 734 nm before testing. The EC_{50} value is calculated which leads to the elimination of 50% ABTS radicals. The ABTS radical scavenging capacity (%) of the tested samples were calculated by the following equation:

$$ABTS\ radical\ scavening\ activity(\%) = (1 - \frac{A1 - A2}{A0}) \times 100$$

Where *A*0 was the absorbance of the blank group (distilled water + ABTS), *A*1 was the absorbance of the sample reaction (sample + ABTS), and *A*2 was the back ground absorbance of the sample.

2.4.3. Ferric ion reducing antioxidant power (FRAP) assay

Reducing power was estimated by FRAP method [2, 13] with minor modifications. In brief, 180 μL of the FRAP working solutions and 5 μL of each sample dilution were mixed in a 96-well plate and then they were incubated for 5 min at 37 °C. Then the absorbance of 593 nm was measured by the Synergy HT Multiscan Spectrum (Bio Tek Instruments, USA).

2.4.4. Ferrous ion chelating assay

The chelating effect on Fe^{2+} ions was measured according to the reference

method [14] with some modifications. Briefly, 1 mL sample was mixed with 3.7 mL of methanol, then the mixture was reacted with ferrous chloride (2 mmol/L, 0.1 mL) and ferrozine (5 mmol/L, 0.2 mL) for 20 min at room temperature to read the absorbance at 562 nm. The chelating activity of the ferrous ion was calculated by the following equation:

$$Chelating\ activity(\%) = \left(1 - \frac{Ab}{As}\right) \times 100$$

Where *A*b is the absorbance of the blank and *A*s is the absorbance in the presence of polysaccharide.

2.5. Structural characterization

2.5.1. Determination of molecular weight (Mw)

The *Mw* of IPS fractions were determined by High Performance Gel Permeation Chromatography (HPGPC) with a Waters 1525 high performance liquid chromatography (HPLC) system (Waters Co. Ltd., Milford, MA, USA) equipped with a model 2410 refractive index detector. The column was eluted with double-distilled water at a flow rate of 0.8 mL/min. Standard dextrans (1.26, 3, 4.32, 10, 40, 70, 100, 380 and 500 kDa, Sigma, USA) were used for molecular weight measurement [15].

2.5.2. Analysis of monosaccharide compositions

The monosaccharide compositions of IPS fractions were determined by HPLC after pre-column derivatization according to a previously established method [16, 17]. The polysaccharide fractions (20 mg) were hydrolyzed with 2 M trifluoroacetic acid (TFA) aqueous solution (5 mL) at 120 ^{o}C for 6 h. Excess TFA was removed by 0.3 mol/L of NaOH (100 μL), then 0.5 mol/L of methanol solution (200 μL) of 1-phenyl-

3-methyl-5-pyrazolone (PMP) was added. After derivatization, the solution was cooled to room temperature followed by adjustment of pH to neutral and then distilled water was added by vigorously shaking. Finally, the mixture was extracted with chloroform for three times and filtered. The resulted solution (10 μL) was injected onto a C_{18} column (4.6 mm × 250 mm) connected with a DAD-UV detector (Agilent Technologies, USA). The mobile phase was a mixture of 0.1 mol/L KH_2PO_4 (pH 6.9)–acetonitrile (89:11) at a flow rate of 1.0 mL/min. Sugar was identified by comparison with reference monosaccharides. Calculation of the molar ratio of monosaccharides was based on the peak area of the monosaccharides investigated.

2.5.3. Infrared spectral analysis

Each fraction of IPS was respectively grounded with dried KBr powder and then pressed into a polymer film for Fourier Transform Infrared Spectroscopy (FTIR) (Thermo Nicolet Co., USA) measurement in a range of 4000-400 cm^{-1}. The major peaks (intensity and wavenumber) were identified and analyzed using the instrument software (EZ OMNIC 6.0, Thermo Electron Corporation, USA).

2.5.4. NMR spectroscopy analysis

Each fraction of IPS was respectively dried using P_2O_5 in vacuum for 4 d, and then 50 mg samples were exchanged with 1 mL D_2O for three times, respectively. The ^1H and ^{13}C NMR spectra were recorded on a Bruker Advance DPX-500 spectrometer at 27 ^oC.

2.6. Cellular antioxidant activity (CAA) test of polysaccharide

2.6.1. Cell culture and cytotoxicity assay

The HepG2 cells were cultured in DMEM medium which contained 10% FBS sup-

plemented with 2 mM L-glutamine and 1% penicillin-streptomycin solution at 37 ^{o}C and 5% CO_2 atmosphere. After 24 h incubation in a 96-well plate (1×10^4 cells/well), the cells were cultured in the presence of different concentrations of polysaccharide solutions for 12 h. After incubation, the MTT test was used to evaluate polysaccharide cytotoxicity in HepG2 [18]. The absorbance at 490 nm was tested by the Synergy HT Multiscan Spectrum. The cell viability was calculated by the following equation:

$$Cell\ vaibility(\%) = \frac{Asample}{Acontrol} \times 100\%$$

2.6.2. Cellular antioxidant activity (CAA) test of polysaccharide

The cellular antioxidant activity (CAA) test was conducted as described previously by Wolfe and Liu [19]. The HepG2 cells were seeded at the density of 1×10^4 cells/well in a transparent, flat-bottomed, and sterile 96-well (Corning, USA) in 100 μL DMEM complete medium. After 24 h culture, 100 μL of IPS-III fractions solutions (200, 400, 600, 800, 1000, 1500 and 2000 μg/mL) were added to incubated for another 6 h, and the quercetin was added in the positive control group. After that, DCFH-DA with final concentration of 25 μM was added and the cells were cultured for 1 h sequentially. After the medium removed and washed by DMEM, the 96-well microplate was placed into a Fluoroskan Ascent FL plate-reader (Thermo Labsystems, Franklin, MA) at 37 ^{o}C, then 100 μL AAPH (600 μM) dissolved in PBS was automatically added at 37 ^{o}C. Emission at 538 nm was measured with excitation at 485 nm every 5 min for 1 h. The CAA unit was calculated as follow:

$$CAA\ units = \left(1 - \frac{\int SA}{\int CA}\right) \times 100$$

where ∫SA is the integrated area under the sample fluorescence versus time curve and

∫CA is the integrated area from the control curve. The CAA value of polysaccharide was denoted as μmol of quercetin equivalents (QE) 100 g^{-1}.

2.7. H_2O_2-induced oxidative damage and the protection by polysaccharide on HepG2 cells

2.7.1. Cell culture and treatment condition

The H_2O_2-induced oxidative damage and the protection by IPS-III fractions on HepG2 cells test was conducted as described previously with minor modifications [20]. The HepG2 cells were seeded at the density of 1×10^4 cells/well on 96-well microplate (Corning, USA) in 100 μL DMEM complete medium. After cultivation for 24 h, the growth medium was removed and hydrogen peroxide was added into the experimental group and sequentially incubated for 2, 4, 6, 8, 12, or 24 h. The MTT test was used to evaluate the cell viability. Then the optimal concentration of hydrogen peroxide and induced incubation time were chosen when the cell viability was close to 50%.

The protective effects of polysaccharides on the oxidative damaged HepG2 cells induced by H_2O_2 was conducted. The HepG2 cells were cultivated at the density of 1×10^4 cells/well in a 96-well plate for 24 h. The supernatant was removed and 100 μL fresh medium with polysaccharide samples at different concentration were added into the protection groups respectively incubating for 8 h. Then H_2O_2 solution with the optimal concentration was added into the damaged and protection groups and sequentially incubated for the optimal time, lastly the cell viability was detected.

2.7.2. DAPI staining

DAPI staining (Sangon Biotech, Shanghai, China) was used to investigate the

protection of IPS-III on H_2O_2-damaged HepG2 cells. In brief, at the end of incubation as described in 2.7.1, 50 μg/L DAPI staining solutions were added and incubated with HepG2 cells for 30 min at 37 ℃ in the dark, followed by washing with PBS for several times. Then, the cells were observed under fluorescence microscope (Nikon eclipse 80i, Japan) with the light of Nikon INTENSILIGHT C-HGFI. The image analysis software was NIS-Elements.

2.7.3. Intracellular ROS measurement

Intracellular ROS was estimated by using a fluorescent probe, 2',7'-dichlorodihydrofluorescein diacetate (DCFH-DA) (Sigma-Aldrich, MO, USA) [21]. In brief, at the end of incubation as described in 2.7.1, the medium was removed and washed with PBS. Finally DCFH-DA (final concentration 5 μM) was added in the dark and incubated at 37 ℃ for 30 min. Then the medium was removed and washed twice with PBS. The DCF fluorescence intensity was detected at 37 ^{o}C with an excitation wavelength of 485 nm and an emission wavelength of 530 nm. The percentage increase in fluorescence per well was calculated by the following formula:

$$Intracellular\ ROS\ production(\%) = \frac{Ft30 - Ft0}{Ft0} \times 100$$

Where *F*t0 is the fluorescence at 0 min and *F*t30 is the fluorescence at 30 min in HepG2 cells exposure to H_2O_2.

2.7.4. Determination of antioxidant related enzymes in H_2O_2-induced HepG2 cells

HepG2 cells were cultured in 6-well plates (1×10^6 cells/well) for 24 h. When the treatment was done, 500 μL of cell lysis buffer was added into each well on ice lysed for 10 min. After centrifuged for 10 min at 12,000 rpm (4 ^{o}C), the liquid supernatant was obtained and cold standby at 4 ^{o}C. The intracellular activities of T-SOD and CAT,

and the content of GSH-Px and MDA were measured using assay kits. Protein concentrations in cell lysates were determined using the BCA method to normalize. The assay results were given in units of enzymatic activity per milligram of protein (U/mg prot).

2.8. Statistical analyses

All data were expressed as the mean ± SD. The determinations were based on three replicate samples. The statistical significance was determined by one-way analysis of variance (ANOVA) followed by Duncan's multiple range test. Values of $p < 0.05$ were considered as statistically significant.

3. Results

3.1. Comparative antioxidant activities evaluation of PFB, IPS and EPS

The DPPH scavenging activities of PFB, EPS and IPS extracted from ABSC had a positive direct correlation with the increasing concentrations of samples, but all of them showed weaker effects on scavenging DPPH radical than Trolox (**Fig. 1A**). Within the range of tested concentrations, the EC_{50} values of PFB, EPS, IPS and Trolox were 0.31 ± 0.02 mg/mL, 0.32± 0.05 mg/mL, 0.08 ± 0.01 mg/mL and 0.06± 0.00 mg/mL, respectively, indicating that IPS had superior effects in scavenging DPPH radicals than PFB and EPS. The ABTS scavenging rate of all the extracts increased with the dose increasing as shown in **Fig. 1B**, but all of these three kinds of polysaccharide demonstrated weak ABTS scavenging capacities when compared with the Trolox. At a concentration of 10.0 mg/mL, IPS was found to have the maximum ABTS scavenging rate (up to 43.83±4.13%). For PFB and EPS, they even showed

much weaker ABTS scavenging capacities. There are positive direct correlation between the FRAP values of PFB, EPS and IPS extracted from ABSC and concentrations (**Fig. 1C**). The results exhibited that the three types of polysaccharide possessed the Fe^{2+} reducing capacity, but all of them were not as strong as Trolox. The Fe^{2+} reducing power of EPS was found to be higher than that of PFB and IPS, and the Fe^{2+} reducing powers of PFB, EPS and IPS increased to 0.20 ± 0.02 mM, 0.25 ± 0.01 mM and 0.34 ± 0.01 mM, respectively, as the concentration increased to 10 mg/mL.

The ferrous ion chelating abilities of PFB, EPS and IPS were found to be positively correlated with the linear dose, but they showed weaker ferrous ion chelating ability when compared with EDTA. The data indicated that PFB and IPS showed stronger ferrous ion chelating abilities than EPS (**Fig. 1D**). The EC_{50} of the ferrous ion chelating abilities of PFB, IPS and EDTA were 1.22 ± 0.02 mg/mL, 1.88 ± 0.05 mg/mL and 0.05 ± 0.00 mg/mL, respectively, indicating that PFB had stronger ferrous ion chelating ability than IPS.

Combining the four assaying data of three samples, it was concluded that IPS extract offered stronger antioxidant properties in *vitro* ($P < 0.05$). Further study should focus on investigating the structural characteristics of IPS to explore the relationship between their antioxidant activities and the structures.

3.2. Monosaccharide composition analysis of IPS

It was found that IPS is composed of three polysaccharides fractions (IPS-I, IPS-II and IPS-III) with the *Mw* of 30.4 kDa (46.1%), 9.7 kDa (35.5%) and 3.1 kDa (18.4%), respectively, as published before (the HPGPC chromatograms of IPS fractions presented in **Fig. S1**). The chromatogram of a standard mixture of eight monosaccharides was shown in **Fig. 2**. The results (**Fig. 2**) indicated both IPS-I and IPS-II consisted of

mannose, rhamnose, glucose and galactose with a molar ratio of 1.3:0.2:4.8:0.8 and 1.5:0.4:60.2:1.0, respectively. IPS-III consisted of mannose, glucose and galactose with a molar ratio of 0.1:5.2:0.1. It is clearly revealed that the most predominant monosaccharide in the analyzed IPS was D-glucose (approximately 97.87%).

3.3. FT-IR spectra analysis of IPS fractions

The structure of three IPS fractions was detected by FT-IR and recorded in region 4000–400 cm^{-1} (**Fig. 3**). IPS-I, IPS-II and IPS-III displayed similar FTIR spectra at the range of 4000–400 cm^{-1}. The absorption peaks between 3400–3200 cm^{-1} were assigned to O-H stretching vibration, and the peaks observed at around 2950 cm^{-1} was attributed to the C-H stretching and bending vibrations of free sugars [22]. The signals at 1630-1625 cm^{-1} reflected the absorption of C=O or C-C groups in uronic acid [15]. The signals at 1400-1420 cm^{-1} were attributed to the bending vibration of C-H, and the signals at 1040-1035 cm^{-1} were attributed to ring vibrations overlapped with stretching vibrations of the C-O-H side groups and the C-O-C glycosidic bond vibration [23]. The characteristic bands of IPS-I, IPS-II and IPS-III were presented at around 1078 cm^{-1}, which was possibly due to the stretching vibration of C-O at the C-4 position of the glucose residue in samples [24].

3.4. NMR spectra analysis

The chemical shifts at 5.73 ppm and at δ 4.60 ppm in ^{1}H NMR spectrum of IPS-I (**Fig. S2**) were corresponded to the anomeric protons that were related with glycosidic bonds with α and β form lingkage, respectively [25]. The chemical shifts at 3.50 ppm and 3.41 ppm are assigned to the H-2 to H-5 protons. IPS-I contains 4 anomeric protons with chemical shifts at 5.86 ppm, 5.73 ppm, 5.11 ppm and 4.60 ppm, respectively. Correspondly, IPS-I also contains 4 anomeric carbon with chemical

shifts at 97.74 ppm, 94.07 ppm, 91.42 ppm and 90.27 ppm, respectively (**Fig. 4A**). In the anomeric region of ^{13}C NMR spectrum of IPS-I (**Fig. 4B**), the signals from δ 74.38 to 70.71 ppm showed the existence of C-2, C-3 and C-4, indicating the presence of α-1-glucoside bonds [26]. Signals at δ 67.49 ppm were due to C-6, indicating the presence of α-1-glucoside bonds and α-1,6-glucoside bonds in IPS-I [27]. There is a chemical shifts at 58.68 ppm that belongs to methoxy signal, and methyl signals also appeared at 14.91 ppm, these signals indicates the existence of heteropolysaccharide. In combined with the results of monosaccharide composition analysis, FT-IR and NMR measurements, these findings indicate that IPS-I had a backbone of (1→6)-α-D-glucopyranosyl residues, and its branched chain is connected by (1→6)-glycosidic linkage with (1 → 6)- α-D-galactopyranosyl residues, (1→3,6)-α-D-mannopyranosyl residues and (1 → 2,3)-β- D-galactose residues.

The chemical shifts at 4.47 ppm in ^{1}H NMR spectrum of IPS-II indicated that the pyranose residue presented in glycosidic linkage was β form (**Fig. 5A**). The chemical shifts from δ 4.45 ppm to 3.97 ppm in ^{1}H NMR spectrum of IPS-II were assigned to protons from C-2 to C-6 in the residues. The ^{1}H NMR spectrum of IPS-II exhibited signals at 4.18 ppm and 3.42 ppm due to CH2-O and CH-O groups of sugars, and the two chemical shifts also are assigned to the H-2 to H-6 protons. The signals at 98.58 ppm in the ^{13}C NMR spectrum of IPS-II demonstrated that there was also α form glucosyl linkage and such signals was attributed to (1→4,6)-α-D-galactopyranosyl in ^{13}C NMR spectrum of IPS-II (**Fig. 5B**) [28]. The signals presented from 70.27 ppm to 72.12 ppm indicated the existence of C-2, C-3 and C-4, showing the presence of α-1,3-glucoside bonds. The chemical shifts at 59.59 ppm and 15.75 ppm indicated the existence of heteropolysaccharide. In conclusion, IPS-II fraction possibly had a backbone of (1→4,6)-D-galactopyranosyl joined by α-D-pyranose or β-D-pyranose with

(1→6)-β-D-mannopyranosyl residues and the (1→3)-α- rhamnose linkages in the side chain.

The ^{1}H and ^{13}C NMR spectra of IPS-III were demonstrated in **Fig. 6.** The chemical shifts at δ 4.23 ppm in ^{1}H NMR spectrum (**Fig. 6A)** were corresponded to anomeric protons with α-configuration. The chemical shifts ranged from δ 4.23 ppm to 3.90 ppm in ^{1}H NMR spectrum of IPS-III (**Fig. 6B**) were assigned to protons from C-2 to C-6 in the residues [27]. The signals at 2.51–2.07 ppm in ^{1}H NMR spectrum suggested the trace of $–CH_2–C(=O)-OH$. The chemical shift at 95.08 ppm was attributed to α-anomeric carbon. The signals presented from 70.07 ppm to 75.13 ppm indicated the existence of C-2, C-3 and C-4, showing the presence of α-1,3-glucoside bonds. In particular, based on these data above, we concluded that IPS-III contained (1→6)-α-D-glucopyranosyl residues and (1→3, 6)-α-D-mannopyranos residues, and its branch consisted of (1 →6)-α-D-galactopyranosyl residues.

3.5. Comparative antioxidant activities assay of IPS-I, IPS-II and IPS-III in vitro

There were positive direct correlation between the samples concentrations and the DPPH scavenging activities of IPS-I, IPS-II and IPS-III fractions (**Fig. 7A**). At the concentration of 10 mg/mL, the DPPH scavenging activities of IPS-I increased to the highest value, up to 87.83± 0.61%. Within the range of tested concentrations, the EC_{50} values of IPS-I, IPS-II and IPS-III were 17.43 ± 1.53 mg/mL, 9.02 ± 0.40 mg/mL and 4.53 ± 0.12 mg/mL, respectively, indicating that IPS-III showed superior effects in scavenging DPPH radicals than IPS-I and IPS-II. The ABTS scavenging activities of IPS-I, IPS-II and IPS-III fractions increased with the increasing of concentrations as shown in **Fig. 7B**, but all of them revealed weak ABTS scavenging capacities. At a concentration of 10 mg/mL, the ABTS scavenging rates of IPS-I, IPS-II and IPS-III

fractions even did not increased to 50%, which was coincided with the results in 3.1. The IPS-I, IPS-II and IPS-III fractions possessed weak Fe^{2+} reducing capacities with low FRAP values (**Fig. 7C**). The FRAP values of IPS-I, IPS-II and IPS-III were only increased to 0.09 ± 0.01 mM, 0.12 ± 0.01 mM and 0.12 ± 0.01 mM, respectively, at the concentration of 10 mg/mL. The ferrous ion chelating abilities of IPS-I, IPS-II and IPS-III fractions showed positive direct correlations with the increasing of samples concentrations (**Fig. 7D**). The EC_{50} values of the ferrous ion chelating abilities of IPS-I, IPS-II and IPS-III fractions were 17.43 ± 1.53 mg/mL, 9.02 ± 0.40 mg/mL and 4.53 ± 0.11 mg/mL, respectively, indicating that IPS-III had stronger ferrous ion chelating ability than IPS-I and IPS-II. The results of the four assays above indicated that IPS-III showed stronger antioxidant properties in *vitro* than IPS-I and IPS-II fractions, so the cellular antioxidant activity of IPS-III in HepG2 cell and its protection effect on H_2O_2-induced oxidative damage HepG2 cells were further investigated.

3.6. Cytotoxicity and cellular antioxidant activity of IPS-III in HepG2 cell

Based on the above data, we further evaluated the antioxidant activity of IPS-III in model cells. **Fig. 8A** shows the cytotoxicity of IPS-III on HepG2 cells, after 12 h treatment of different concentrations of IPS-III (50-4000 μg/mL), the results of MTT assay showed that IPS-III didn't exhibit cytotoxic effects on HepG2 cells. IPS-III can reduce the increasing trend of fluorescence (**Fig. 8B-E**). It is obvious that the inhibition of cellular oxidative capacity of IPS-III (200–1000 μg/mL) was concentration dependent. When the IPS-III concentration increase to 1500 and 2000 μg/mL, the CAA unit tended to decrease. The highest CAA unit was calculated as 48.01 ± 0.98, which did not achieve 50. The CAA data implied that IPS-III has the antioxidant activity inside HepG2 cells.

3.7. The protection of IPS-III on H_2O_2-damaged HepG2 cells

H_2O_2 can be directly converted to hydroxyl radical and oxygen free radical and it could induce oxidative stress in HepG2 cells in this experiment. As shown in **Fig. 9A**, H_2O_2 could induce oxidative damage on HepG2 cells and the damage was time- and concentration-dependent. The cell viability achieved 52.61 ± 5.55% in treatment group with H_2O_2 treatment (1200 μM) for 8 h, and further validation experiment indicated that such condition was stable and repeatable.

The protective effects of IPS-III on H_2O_2-damaged HepG2 cells were shown in **Fig. 9B**. IPS-III treatment improved the cell viability compared with the H_2O_2-damaged cell without IPS-III treatment. With the increasing of incubation time (from 4 h to 12 h), the cell viability of H_2O_2-damaged HepG2 cells treated with IPS-III was also improved. Compared with the control group, the cell viability has increased more than 20% in IPS-III treatment group at concentration of 800 and 1000 μg/mL after protecting for 8 h. The H_2O_2-damaged HepG2 cells were well protected by incubation with different IPS-III concentrations (from 200 to 2000 μg/mL), and under such conditions the protective oxidative stress inhibition effect of IPS-III was extremely significant at concentration of 800 μg/mL ($P < 0.01$).

3.8. Effects of IPS-III on cell survival of H_2O_2-induced HepG2 cells

DAPI staining was used for investigation of the effects of the absence (**Fig. 10B-control**) or presence of IPS-III on DNA and nuclear structure in HepG2 cells under H_2O_2-induced oxidative damage. As illustrated in **Fig. 10**, compared with the control group, cells exposure to 1200 μM H_2O_2 for 8 h revealed lots of small bright blue dots, representing chromatin condensation or nuclear fragmentation in the model group. However, the treatments with IPS-III (from 200 to 2000 μg/mL) for 8 h decreased the

nuclear condensation and fragmentation, indicating that IPS-III could prevent HepG2 cells from death under H_2O_2-induced oxidative damage.

3.9. Effects of IPS-III on ROS production in H_2O_2-damged HepG2 cells

To further investigate the effects of IPS-III on protective effects in H_2O_2-induced HepG2 cells, we conducted the determination of ROS formation. As presented in **Fig. 11**, the level of cellular ROS in HepG2 cells incubated with H_2O_2 alone for 8 h was significantly ($P < 0.05$) increased with the mean DCF fluorescence intensity reaching to 157.10% ± 2.35%, implying that ROS was overproduced and accumulated after H_2O_2 incubation. When the H_2O_2-damaged HepG2 cells were protected by IPS-III (from 200 μg/mL to 800 μg/mL), the relative intracellular ROS production was decreased with a dose-dependent manner. When IPS-III (800 μg/mL) was added to protect the H_2O_2-damaged HepG2 cells, ROS production decreased to the lowest level (7.26 ± 1.57), which was 2.03 times low than that of control group. However, when the IPS-III concentration continued to increase from 800 μg/mL to 2000 μg/mL, the intracellular ROS began to accumulate. The results indicated that IPS-III within certain concentrations (from 200 μg/mL to 800 μg/mL) could decease the ROS production in the H_2O_2-damaged HepG2. This finding suggested that H_2O_2-induced cytotoxicity was associated with overproduction of ROS, and IPS-III afforded protection against H_2O_2 stress in HepG2 cells.

3.10. Effects of IPS-III on the related antioxidant enzymes in H_2O_2-damaged HepG2 cells

In this study, we assayed the effects of IPS-III on the intracellular antioxidant enzyme activities of T-SOD, CAT, GSH-Px and MDA in HepG2 cells. When the HepG2 cells were exposed to H_2O_2, the contents of T-SOD was significantly increased in the ex-

periment as compared with the control group ($P < 0.01$), but IPS-III treatment could significantly decrease the T-SOD activities ($P < 0.01$) (**Fig. 12A**). When the IPS-III concentration was 800 μg/mL and 1000 μg/mL, the T-SOD contents in HepG2 cells was significantly decreased to 0.99 ± 0.01 U/mg and 0.96 ± 0.02 U/mg, respectively ($P < 0.01$). As shown in **Fig. 12B**, the CAT levels in HepG2 cells exposed to H_2O_2 was significantly increased 2.56 times high in contrast to the control group (4.49 ± 0.88 U/mg) ($P < 0.01$). After the H_2O_2-induced oxidative damage HepG2 cells were treated with IPS-III (from 200 μg/mL to 2000 μg/mL), the CAT levels decreased significantly ($P < 0.05$). The CAT level was the lowest (only 0.73 ± 0.28 U/mg) at the IPS-III concentration of 800 μg/mL. **Fig. 12C** showed that the GSH-Px levels in the H_2O_2-induced HepG2 cells treated with IPS-III (from 0 μg/mL to 2000 μg/mL) were increased. When the H_2O_2-induced HepG2 cells were treated with 2000 μg/mL of IPS-III, the GSH levels had raised to 14.16 ± 0.89 U/mg, which was close to the control group (14.64 ± 0.89 U/mg). The MDA levels in the H_2O_2-induced HepG2 cells were significantly increased when compared with the control group ($P < 0.01$) (**Fig. 12D**). If the HepG2 cells were exposed to 1200 μM H_2O_2 for 8 h, the MDA levels had increased to 14.72 ± 0.44 μM/mg, whereas the treatment with IPS-III could significantly decrease the MDA levels in the H_2O_2-damaged HepG2 cells ($P<0.01$), and such protective effect was dose dependent. Apparently, the CAT and GSH-Px levels in HepG2 cells incubated by IPS-III were significantly higher than that of the H_2O_2-damaged group, and the HepG2 cells protected by IPS-III had strong antioxidant enzyme activities. It was proved that the IPS-III can protect H_2O_2-damaged HepG2 cells from oxidative stress not only by scavenging intracellular free radicals but also enhancing endogenous antioxidant defense systems.

4. Discussion

There were significant differences of antioxidant activities among PFB, EPS and IPS, and the results showed that IPS possessed the most strongest antioxidant activities than PFB and EPS in *vitro*, its DPPH inhibition reached the highest value of 81.61± 1.62% at 0.75 mg/mL, ABTS inhibition of 43.83±4.13% at 10 mg/mL, and FRAP value of 0.34 ± 0.01 Mm at 10 mg/mL. The relsuts were consistent with the results obtained by other studies. Hao et al. (2016) reported that IPS isolated from *Fomitopsis pinicola*, a kinds of traditional Chinese medicine, showed higher antioxidant potential than EPS with smaller EC_{50} values of significant DPPH inhibition and hydroxyl radical scavenging activity [16]. Zhang et al. (2016) also concluded that the polysaccharides (*Pleurotus eryngii* SI-04) from submerged cultured mycelia showed better scavenging capacity to superoxide anion, DPPH and hydroxyl radicals and when compared with polysaccharides extracted from fruiting bodies [7]. However, when the IPS extrations were undergone a series processes of purifications and separations, its antioxidant activities weakened. For example, the EC_{50} values of IPS extractions was 0.08 ± 0.01 mg/mL, but the EC_{50} values of IPS-I, IPS-II and IPS-III were 17.43 ± 1.53 mg/mL, 9.02 ± 0.40 mg/mL and 4.53 ± 0.12 mg/mL, respectively, which were much higher than that of IPS extractions. The decreasing trends of the antioxidant activities of the purified IPS fractions could be due to the losing of some materials (such as proteins, polyphenols in the crudes polysaccharides) that could coordinate with polysaccharides to improve its antioxidant activity [29]. The significant differences of antioxidant activities among polysaccharides fractions could due to their differences in structure. Researchers suggested that the activity of polysaccharides could be affected by the molecular weights [30]. It was reported that polysaccharides with lower *Mw* (< 100 kDa) have stronger and more significant antioxidant activities than the large ones due to the low apparent viscosity, excellent water-solubility and bio-absorbability

[31]. There is a report that the radical scavenging capacity could be effected by the amount of −OH groups and the present of C-O-Se [32, 7]. Zhang et al. (2016) found that the high content of uronic acid in GLEPS (21.74%) resulted in stronger antioxidant capacities of GLEPS [7]. Since many factors such as monosaccharides composition, their bond types and glycosyl linkages could affect antioxidant activity of polysaccharides, the relationship between the structure of IPS and its antioxidant capability need further study [33].

ROS overproduction is associated with mitochondrial membrane potential collapse (MMP) and excessive mitochondrial lipid peroxidation [34]. Accordingly, the intracellular ROS levels were significantly increased in HepG2 cells after exposure to H_2O_2, which induced lipid peroxidation in the cultured cells as the corresponding increasing levels of MDA. Contrary to the H_2O_2-treated group, significantly lower fluorescence intensity and MDA levels were observed in damaged cells that were pretreated with IPS-III, suggesting that IPS-III may be an protector of endogenous cellular antioxidant defense mechanisms. Our preliminary data indicated that IPS-III was capable of inhibiting H_2O_2-induced excessive ROS production. The decreasing trending of SOD and CAT activities in H_2O_2-induced oxidative damage HepG2 cells protected with IPS-III illustrated that the antioxidant enzymes including SOD, CAT and GSH-Px plays a key role in this process. The concentrations of antioxidants including SOD, CAT and GSH-Px in cells would increase with the acceleration of oxidative stress level, and such process acts as a key role in diverging physiological and pathophysiological conditions such as aging and Parkinson diseases [35]. However, we observed that T-SOD levels in H_2O_2-induced oxidative damage HepG2 cells pretreated with IPS-III tended to decrease in a concentration-dependent manner, and then an increasing trending was observed when the concentration of IPS-III increased to

2000 μg/mL. Such changes could be explained that IPS-III may either accelerate or decrease T-SOD biosynthesis in H_2O_2-induced oxidative damage HepG2 cells, and such process might be dependent on maintenance between the intracellular ROS concentrations and total levels of endogenous and exogenous antioxidants [36].

5. Conclusions

In conclusion, polysaccharides from ABSC were comparatively evaluated for their antioxidant properties. Among the isolated polysaccharides, IPS showed better antioxidant activity than PFB and EPS in *vitro*. Further purification and structure analyses indicated that IPS mainly consisted of three fractions (IPS-I, IPS-II and IPS-III), both IPS-I and IPS-II consisted of mannose, rhamnose, glucose and galactose, while IPS-III consisted of mannose, glucose and galactose. FT-IR and NMR data indicated that IPS was mainly composed of (1→6)-linked α-D-glucose. There are significant differences of antioxidant activities among IPS-I, IPS-II and IPS-III fractions in *vitro*, and IPS-III fraction revealed stronger antioxidant activity than IPS-I and IPS-II. IPS-III also possesses a potent antioxidant ability inside HepG2 cells, and it could protect HepG2 cells from H_2O_2-induced cytotoxicity by scavenging overproduced cellular ROS and inhibiting SOD, CAT and GSH depletion to weaken lipid peroxidation. These findings suggested that IPS-III could be a novel antioxidant and that it could afford protection against H_2O_2-induced cytotoxicity and oxidative stress.

Conflicts of Interest

The authors declare that there is no conflict of interests.

Formatting of funding sources

This work was financially supported by the Natural Science Foundation of China (31960471, 31871904) and the Science and Technology Project of Qianghai (No. 2018HZ801).

References

[1] G. Serviddio, F. Bellanti, G. Vendemiale, Free radical biology for medicine: learning from nonalcoholic fatty liver disease, Free Radic Biol Med. 65 (2013) 952-968.

[2] C. Gao, Y. Wang, C. Wang, Z. Wang, Antioxidant and immunological activity in vitro of polysaccharides from *Gomphidius rutilus* mycelium, Carbohydr. Polym. 92 (2013) 2187-2192.

[3] A.C. Ruthes, E.R. Carbonero, M.M. Córdova, C.H. Baggio, G.L. Sassaki, P.A.J. Gorin, A.R.S. Santos, M. Iacomini, Fucomannogalactan and glucan from mushroom *Amanita muscaria*: Structure and inflammatory pain inhibition, Carbohydr. Polym. 98 (2013) 761-769.

[4] S. Samanta, A.K. Nandi, I.K. Sen, P. Maity, M. Pattanayak, K.S.P. Devi, S. Khatua, T.K. Maiti, K. Acharya, S.S. Islam, Studies on antioxidative and immunostimulating fucogalactan of the edible mushroom *Macrolepiota dolichaula*, Carbohydr. Res. 413 (2015) 22-29.

[5] Q.L. Huang, K.C. Siu, W.Q. Wang, Y.C. Cheung, J.Y. Wu, Fractionation, characterization and antioxidant activity of exopolysaccharides from fermentation broth of a *Cordyceps* sinensis fungus, Process. Biochem. 48 (2013) 380-386.

[6] J. Si, G. Meng, Y. Wu, H.F. Ma, B.K. Cui, Y.C. Dai, Medium composition

optimization, structural characterization, and antioxidant activity of exopolysaccharides from the medicinal mushroom *Ganoderma lingzhi*, Int. J. Biol. Macromol. 124 (2019) 1186-1196.

[7] C. Zhang, S. Li, J. Zhang, C. Hu, G. Che, M. Zhou, L. Jia, Antioxidant and hepatoprotective activities of intracellular polysaccharide from *Pleurotus eryngii* SI-04, Int. J. Biol. Macromol. 91 (2016) 568-577.

[8] Y. Jiao, H. Kuang, J. Hu, Q. Chen, Structural characterization and anti-hypoxia activities of polysaccharides from the sporocarp, fermentation broth and cultured mycelium of *Agaricus bitorquis* (Quel.) Sacc. Chaidam in mice, J. Funct. Foods. 51 (2018) 75-85.

[9] Y. Jiao, H. Kuang, J. Wu, Q. Chen, Polysaccharides from the edible mushroom *agaricus bitorquis* (quel.) sacc. chaidam show anti-hypoxia activities in pulmonary artery smooth muscle cells, Int. J. Macromol. Sci. 20 (2019).

[10] M. DuBois, K.A. Gilles, J.K. Hamilton, P.A. Rebers, F. Smith, Colorimetric Method for Determination of Sugars and Related Substances, Anal. Chem. 28 (1956) 350-356.

[11] K. Shimada, K. Fujikawa, K. Yahara, T. Nakamura, Antioxidative properties of xanthan on the autoxidation of soybean oil in cyclodextrin emulsion, J. Agric. Food. Chem. 40 (1992) 945-948.

[12] K. Kozics, V. Klusová, A. Srančíková, P. Mučaji, D. Slameňová, Ľ. Hunáková, B. Kusznierewicz, E. Horváthová, Effects of Salvia officinalis and Thymus vulgaris on oxidant-induced DNA damage and antioxidant status in HepG2 cells, Food. Chem. 141 (2013) 2198-2206.

[13] F. Radu, H. Bean, C. Schuler, R.E. Leggett, R.M. Levin, Comparative evaluation of antioxidant reactivity between ovariectomized and control urinary bladder tissue

using ferric reducing ability of plasma and cupric ion reducing antioxidant capacity assays, L. U. T. S. 1 (2009) 93-97.

[14] S.A. Ganie, E. Haq, A. Masood, A. Hamid, M.A. Zargar, Antioxidant and protective effect of ethyl acetate extract of *podophyllum hexandrum rhizome* on carbon tetrachloride induced rat liver injury, Evid-Based. Compl. Alt. (2011) 1-12.

[15] Y. He, M. Ye, Z. Du, H. Wang, Y. Wu, L. Yang, Purification, characterization and promoting effect on wound healing of an exopolysaccharide from *Lachnum* YM405, Carbohydrate Polymers. 105 (2014) 169-176.

[16] L. Hao, Z. Sheng, J. Lu, R. Tao, S. Jia, Characterization and antioxidant activities of extracellular and intracellular polysaccharides from *Fomitopsis pinicola*, Carbohydr. Polym. 141 (2016) 54-59.

[17] H.H. Sun, W.J. Mao, Y. Chen, S.D. Guo, H.Y. Li, X.H. Qi, Y.L. Chen, J. Xu, Isolation, chemical characteristics and antioxidant properties of the polysaccharides from marine fungus *Penicillium* sp F23-2, Carbohydr. Polym. 78 (2009) 117-124.

[18] A.D.R.A. Pires, A.C. Ruthes, S.M.S.C. Cadena, A. Acco, P.A.J. Gorin, M. Iacomini, Cytotoxic effect of *Agaricus bisporus* and *Lactarius rufus* β-D-glucans on HepG2 cells, Int. J. Biol. Macromol. 58 (2013) 95-103.

[19] K.L. Wolfe, R.H. Liu, Cellular antioxidant activity (caa) assay for assessing antioxidants, foods, and dietary supplements, J. Agri. Food. Chem. 55 (2007) 8896-8907.

[20] R. Liang, Z. Zhang, S. Lin, Effects of pulsed electric field on intracellular antioxidant activity and antioxidant enzyme regulating capacities of pine nut (*Pinus koraiensis*) peptide QDHCH in HepG2 cells, Food Chem. 237 (2017) 793-802.

[21] H. Wang, J.A. Joseph, Quantifying cellular oxidative stress by dichlorofluorescein assay using microplate reader11Mention of a trade name,

proprietary product, or specific equipment does not constitute a guarantee by the United States Department of Agriculture and does not imply its approval to the exclusion of other products that may be suitable, Free Radic Biol Med. 27 (1999) 612-616.

[22] J. Zhu, W. Liu, J. Yu, S. Zou, J. Wang, W. Yao, X. Gao, Characterization and hypoglycemic effect of a polysaccharide extracted from the fruit of Lycium barbarum L, Carbohydr. Polym. 98 (2013) 8-16.

[23] S. Guo, W. Mao, Y. Li, Q. Gu, Y. Chen, C. Zhao, N. Li, C. Wang, T. Guo, X. Liu, Preparation, structural characterization and antioxidant activity of an extracellular polysaccharide produced by the fungus *Oidiodendron truncatum* GW, Process. Biochem. 48 (2013) 539-544.

[24] K.I. Shingel, Determination of structural peculiarities of dexran, pullulan and gamma-irradiated pullulan by Fourier-transform IR spectroscopy, Carbohydr. Res. 337 (2002) 1445-1451.

[25] J. Li, L. Fan, S. Ding, Isolation, purification and structure of a new water-soluble polysaccharide from Zizyphus jujuba cv Jinsixiaozao, Carbohydr. Polym. 83 (2011) 477-482.

[26] J.K. Yan, Y.Y. Wang, H.L. Ma, Z.B. Wang, J.J. Pei, Structural characteristics and antioxidant activity in *vivo* of a polysaccharide isolated from *Phellinus linteus* mycelia, J. Taiwan. Inst. Chem. E. 65 (2016) 110-117.

[27] P.F. He, L. He, A.Q. Zhang, X.L. Wang, L. Qu, P.L. Sun, Structure and chain conformation of a neutral polysaccharide from sclerotia of *Polyporus umbellatus*, Carbohydr. Polym. 155 (2017) 61-67.

[28] Y. Yu, Y. Li, C. Du, H. Mou, P. Wang, Compositional and structural characteristics of sulfated polysaccharide from Enteromorpha prolifera, Carbohydr.

Polym. 165 (2017) 221-228.

[29] G. Chen, C. Li, S. Wang, X. Mei, H. Zhang, J. Kan, Characterization of physicochemical properties and antioxidant activity of polysaccharides from shoot residues of bamboo (*Chimonobambusa quadrangularis*): Effect of drying procedures, Food. Chem. 292 (2019) 281-293.

[30] L. Zhang, X.L. Li, X.J. Xu, F.B. Zeng, Correlation between antitumor activity, molecular weight, and conformation of lentinan, Carbohydr. Res. 340 (2005) 1515-1521.

[31] R.H. Jason, D.T. Douglas, Nitric Oxide and Cancer Therapy: The Emperor has NO Clothes, Curr. Pharm. Design. 16 (2010) 381-391.

[32] Y. Henrotin, B. Kurz, T. Aigner, Oxygen and reactive oxygen species in cartilage degradation: Friends or foes?, Osteoarthr. Cartilage. 13 (2005) 643-654.

[33] T.C.T. Lo, C.A. Chang, K.H. Chiu, P.K. Tsay, J.F. Jen, Correlation evaluation of antioxidant properties on the monosaccharide components and glycosyl linkages of polysaccharide with different measuring methods, Carbohydr. Polym. 86 (2011) 320-327.

[34] M.T. Lin, M.F. Beal, Mitochondrial dysfunction and oxidative stress in neurodegenerative diseases, Nature. 443 (2006) 787-795.

[35] J.B. Schulz, J. Lindenau, J. Seyfried, J. Dichgans, Glutathione, oxidative stress and neurodegeneration, Eur. J. Biochem. 267 (2000) 4904-4911.

[36] A. Prathapan, S.V. Nampoothiri, S. Mini, K.G. Raghu, Antioxidant, antiglycation and inhibitory potential of Saraca ashoka flowers against the enzymes linked to type 2 Diabetes and LDL oxidation, Eur. Rev. Med. Pharmaco. 16 (2012) 57-65.

Figure captions

Fig. 1. The DPPH radical inhibition (A), ABTS radical inhibition (B), FRAP values (C) and ferrous ion chelating abilities (D) of PFB, EPS and IPS at different concentrations.

Fig. 2. HPLC chromatograph of monosaccharide standards (A), IPS-I (B), IPS-II (C) and IPS-III (D) (1-D-mannose, 2-L-rhamnose, 3-glucuron-ic acid, 4-galacturonic acid, 5-D-glucose, 6-D-galactose, 7-D-xylose, 8-L-arabinose).

Fig. 3. FT-IR spectrum of IPS-I, IPS-II and IPS-III from ABSC.

Fig. 4. The DPPH radical inhibition (A), ABTS radical inhibition (B), FRAP values (C) and ferrous ion chelating abilities (D) of IPS-I, IPS-II and IPS-III at different concentrations.

Fig. 5. ^{1}H NMR spectrum of IPS-I (A); ^{13}C NMR spectrum of IPS-I (B). The red line: Spectrum; the green line: Integral, and the numbers in blue corresponding to its integral values; the numbers in purple: multiplets.

Fig. 6. ^{1}H NMR spectrum of IPS-II (A); ^{13}C NMR spectrum of IPS-II (B). The red line: Spectrum; the green line: Integral, and the numbers in blue corresponding to its integral values; the numbers in purple: multiplets.

Fig. 7. ^{1}H NMR spectrum of IPS-III (A); ^{13}C NMR spectrum of IPS-III (B). The red line: Spectrum; the green line: Integral, and the numbers in blue corresponding to its integral values; the numbers in purple: multiplets.

Fig. 8. The cellular antioxidant activity (CAA) assay of IPS-III in HepG2 cell. (A) The results of MTT assay in *vivo*. 50-4000 μg/mL IPS-III were applied on HepG2 cells. The * and ** on the top of the bar means the significances vs the control group ($P < 0.05$ and $P < 0.01$, respectively). (B-C) 0-2000 μg/mL IPS-III and 1-15 μM of quercetin reduced the DCF fluorescence time-dependently. (D-E) The regression of

the dose–response curve of IPS and quercetin were shown. *y* is the CAA units; *x* is the concentration of sample. The effective concentration (EC_{50}) was calculated.

Fig. 9. Damage effect of H_2O_2 on HepG2 cells (A) and protective effect of IPS-III on H_2O_2-induced oxidative damage (exposure to 1200 μM H_2O_2 for 8 h) in HepG2 cells (B). Vertical bars indicate mean values ± SD.

Fig. 10. Effects of IPS-III on cell survival of HepG2 cells under H_2O_2-induced oxidative damage by DAPI staining method. A: Control conditions. B: After exposure to 1200 μM H_2O_2 for 8 h. C: IPS-III (200 μg/mL) + H_2O_2; D: IPS-III (400 μg/mL) + H_2O_2; E: IPS-III (600 μg/mL) + H_2O_2; F: IPS-III (800 μg/mL) + H_2O_2; G: IPS-III (1000 μg/mL) + H_2O_2; H: IPS-III (1500 μg/mL) + H_2O_2; I: IPS-III (2000 μg/mL) + H_2O_2.

Fig. 11. The effect of IPS-III on ROS production in H_2O_2-induced HepG2 cells.

Fig. 12. The effect of IPS-III on T-SOD (A), CAT (B), GSH-Px (C) and MDA (D) in H_2O_2-induced HepG2 cells.

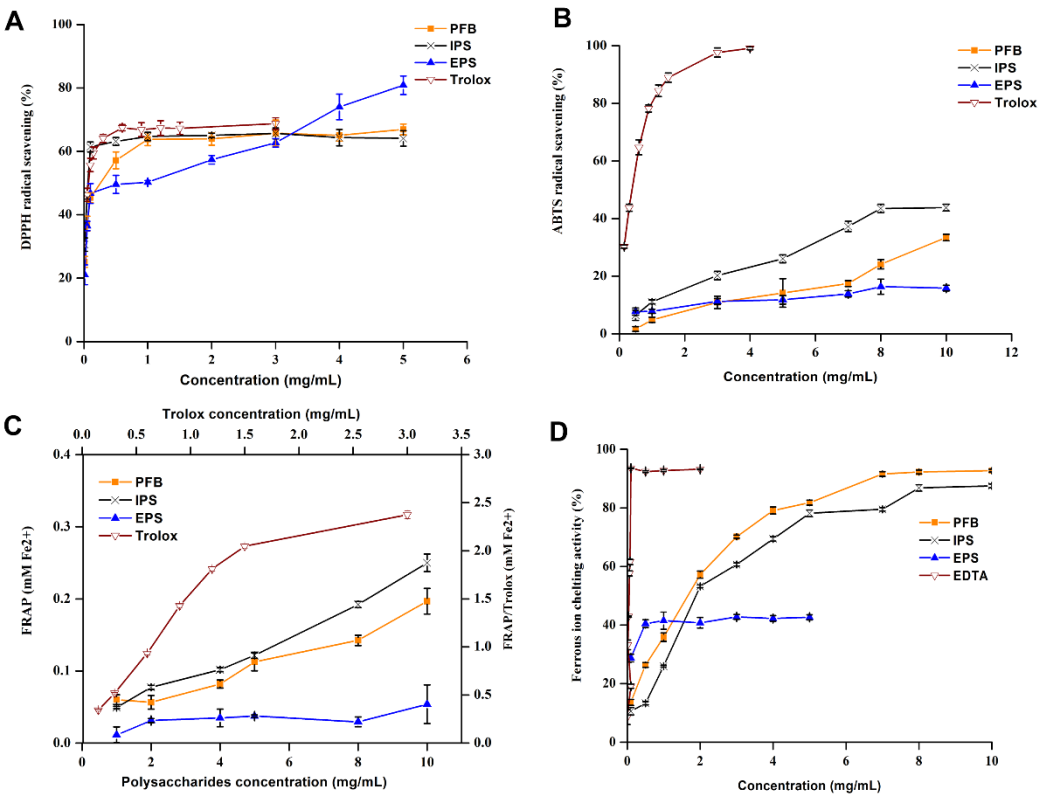

Fig. 1. The DPPH radical inhibition (A), ABTS radical inhibition (B), FRAP values (C) and ferrous ion chelating abilities (D) of PFB, EPS and IPS at different concentrations.

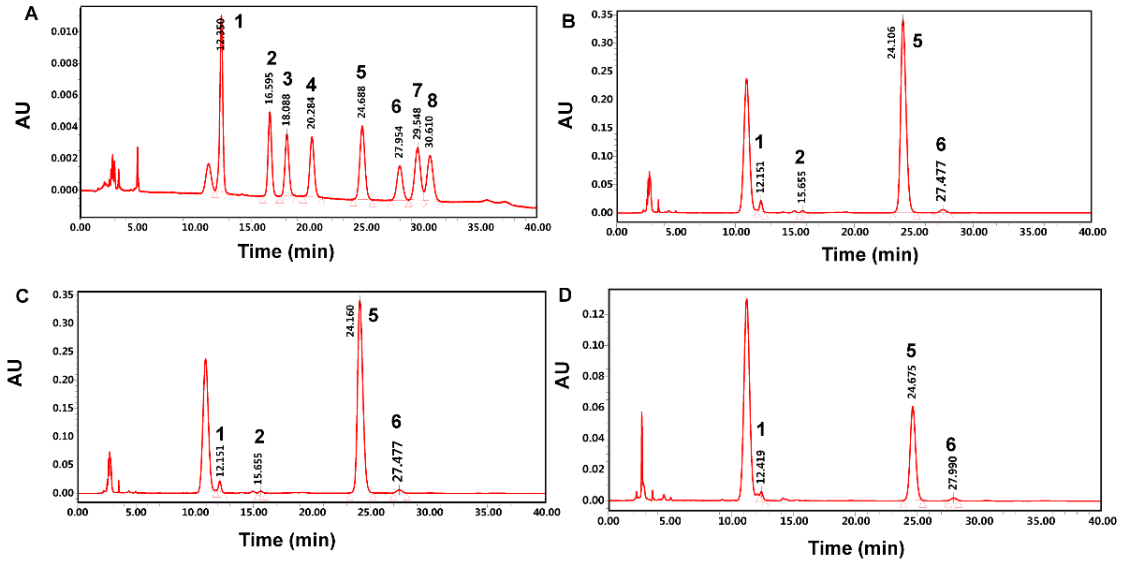

Fig. 2. HPLC chromatograph of monosaccharide standards (A), IPS-I (B), IPS-II (C) and IPS-III (D) (1-D-mannose, 2-L- rhamnose, 3-glucuron-ic acid, 4-galacturonic ac-id, 5-D-glucose, 6-D-galactose, 7-D-xylose, 8-L-arabinose).

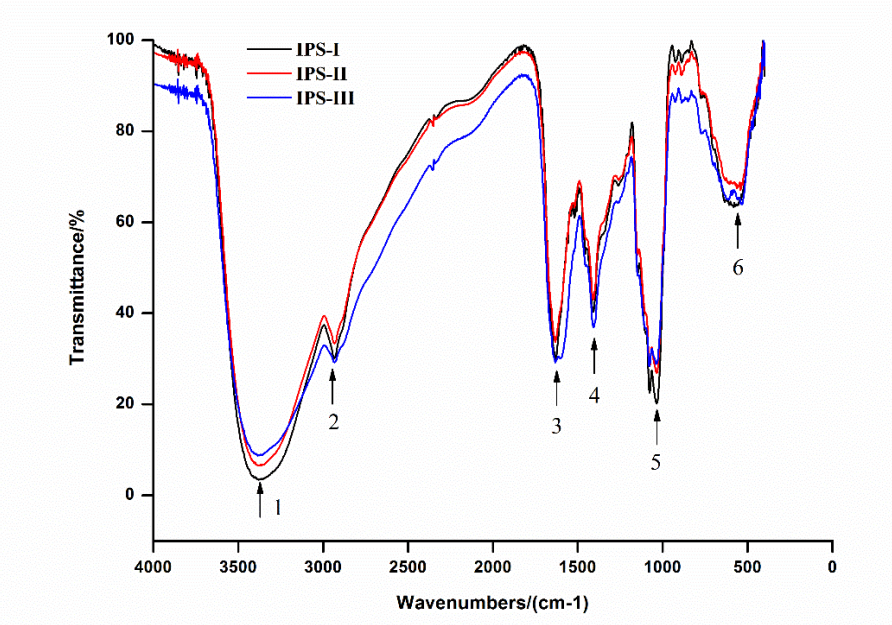

Fig. 3. FT-IR spectra of IPS-I, IPS-II and IPS-III from ABSC.

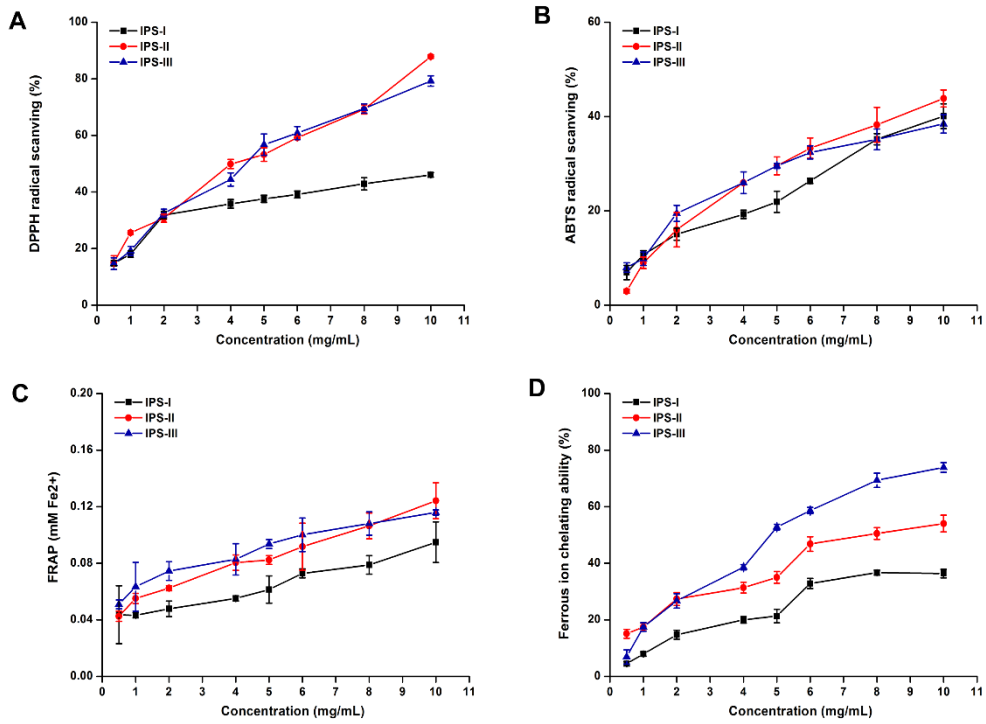

Fig. 4. The DPPH radical inhibition (A), ABTS radical inhibition (B), FRAP values (C) and ferrous ion chelating abilities (D) of IPS-I, IPS-II and IPS-III at different concentrations.

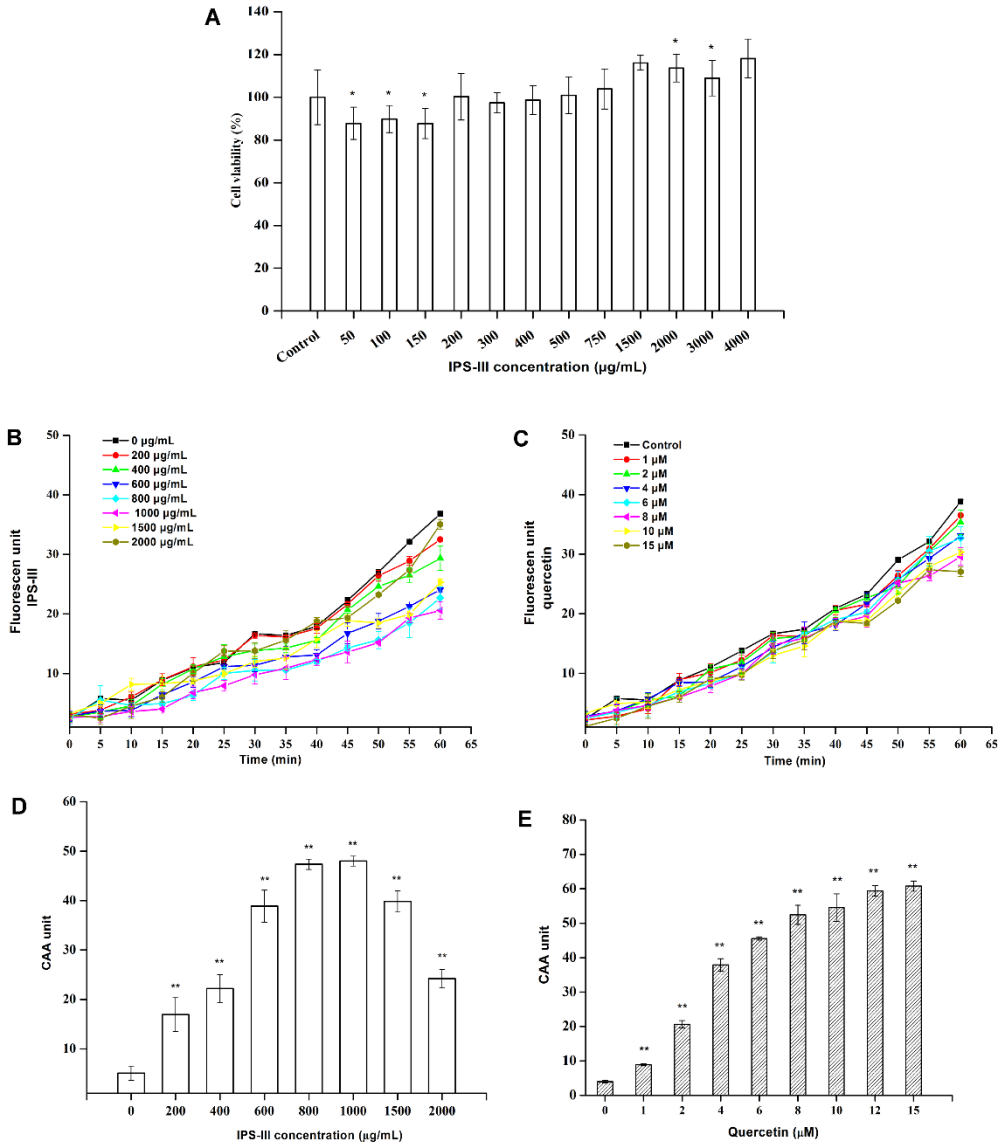

Fig. 5. The cellular antioxidant activity (CAA) assay of IPS-III in HepG2 cell. (A) The results of MTT assay in *vivo*. 50-4000 μg/mL IPS-III were used to treat HepG2 cells. * and ** on the top of the bar means the significances vs the control group ($P < 0.05$ and $P < 0.01$, respectively). (B-C) 0-2000 μg/mL IPS-III and 1-15 μM of quercetin reduced the DCF fluorescence time-dependently. (D-E) The regression of the dose–response curve of IPS and quercetin were shown. *y* is the CAA units; *x* is the concentration of sample. The effective concentration (EC_{50}) was calculated.

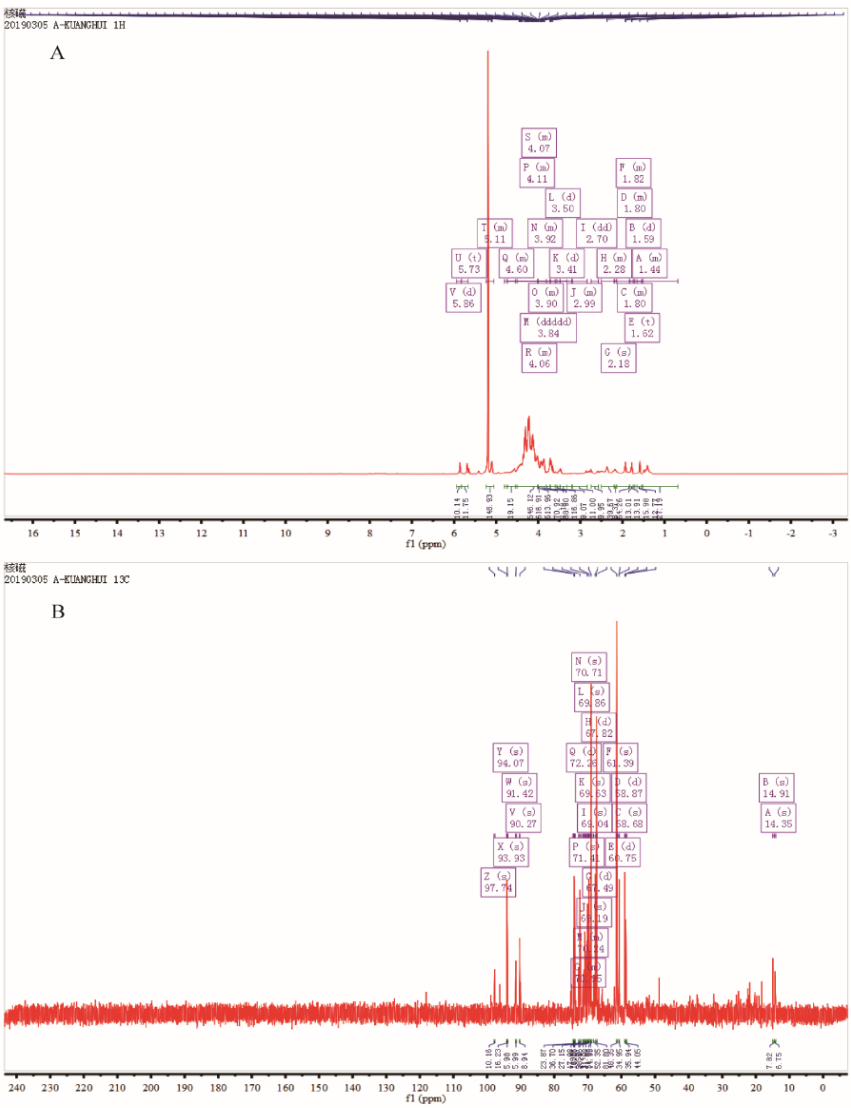

Fig. 6. ^{1}H NMR spectrum of IPS-I (A); ^{13}C NMR spectrum of IPS-I (B). The red line: Spectrum; the green line: Integral, and the numbers in blue corresponding to its integral values; the numbers in purple: multiplets

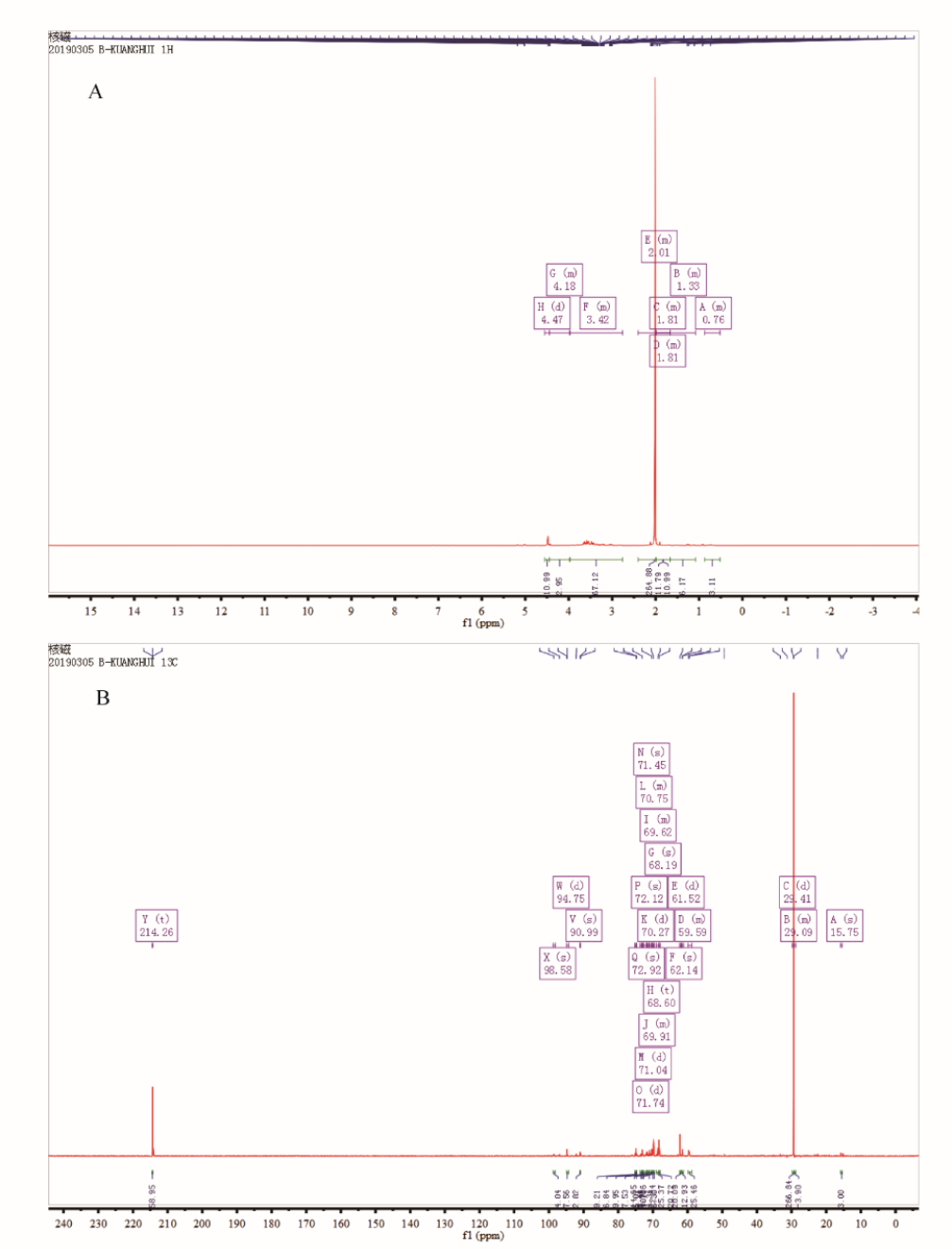

Fig. 7. ^{1}H NMR spectrum of IPS-II (A); ^{13}C NMR spectrum of IPS-II (B). The red line: Spectrum; the green line: Integral, and the numbers in blue corresponding to its integral values; the numbers in purple: multiplets

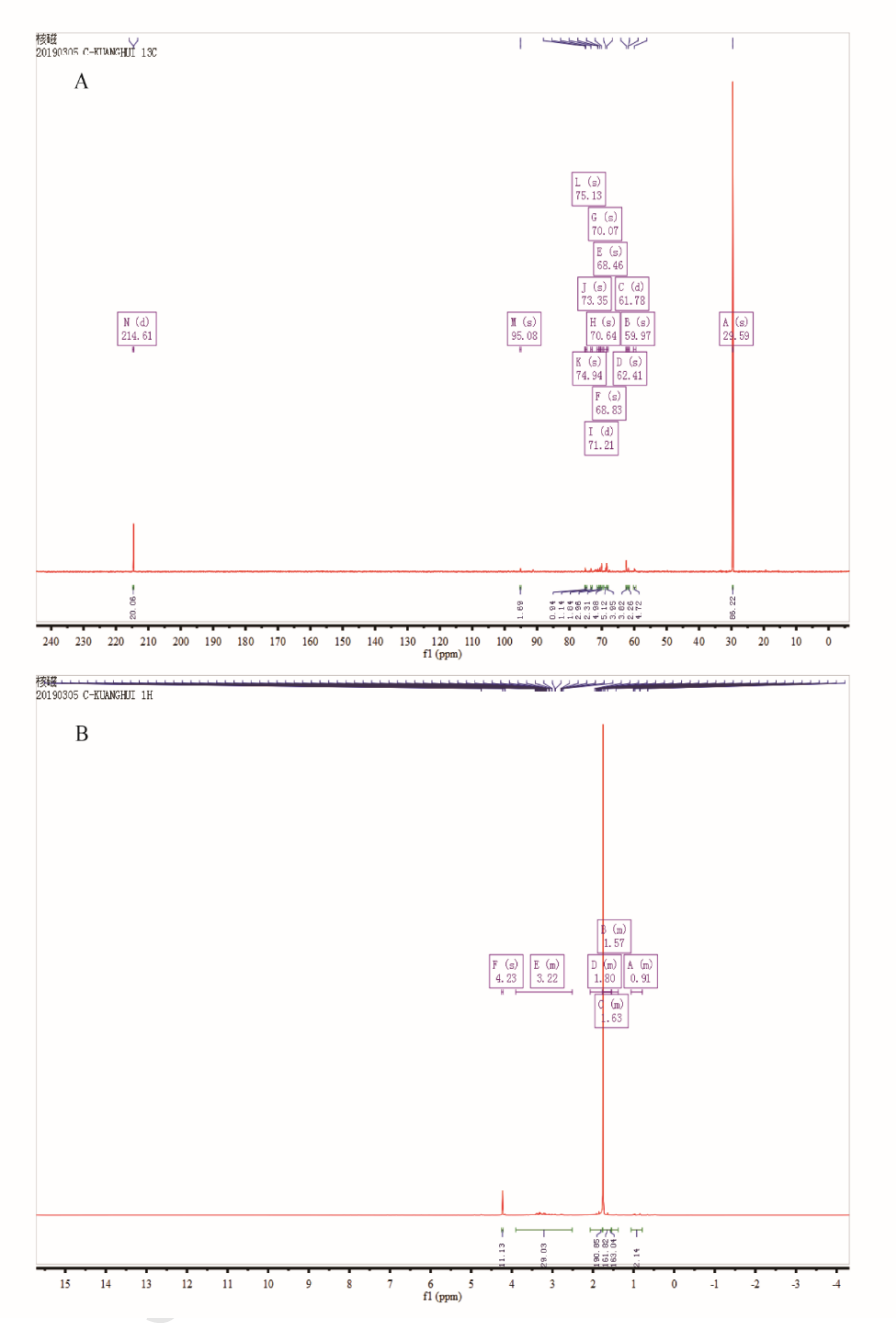

Fig. 8. ^{1}H NMR spectrum of IPS-III (A); ^{13}C NMR spectrum of IPS-III (B). The red line: Spectrum; the green line: Integral, and the numbers in blue corresponding to its integral values; the numbers in purple: multiplets.

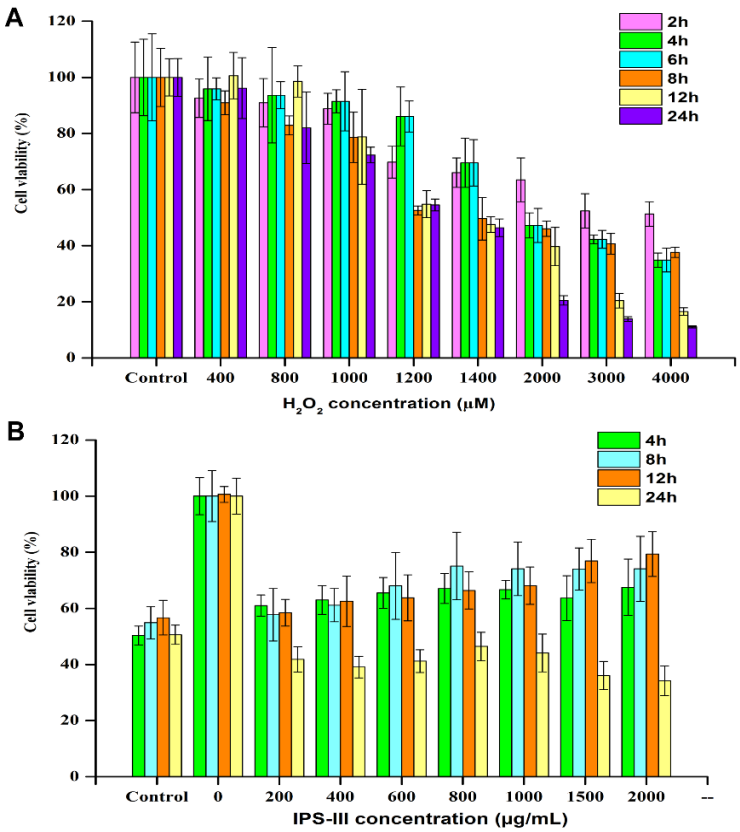

Fig. 9. Damage effect of H_2O_2 on HepG2 cells (A) and protective effect of IPS-III on H_2O_2-induced oxidative damage (1200 μM H_2O_2 for 8 h) in HepG2 cells (B). Vertical bars indicate mean values ± SD.

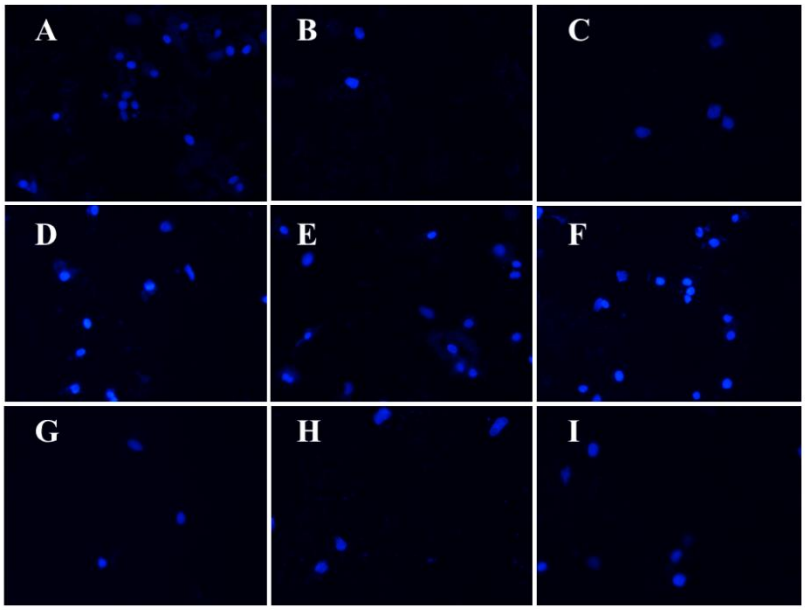

Fig. 10. Effects of IPS-III on the cell survival of HepG2 cells under H_2O_2-induced oxidative damage by DAPI staining method. A: Control conditions. B: After exposure to 1200 μM H_2O_2 for 8 h. C: IPS-III (200 μg/mL) + H_2O_2; D: IPS-III (400 μg/mL) + H_2O_2; E: IPS-III (600 μg/mL) + H_2O_2; F: IPS-III (800 μg/mL) + H_2O_2; G: IPS-III (1000 μg/mL) + H_2O_2; H: IPS-III (1500 μg/mL) + H_2O_2; I: IPS-III (2000 μg/mL) + H_2O_2.

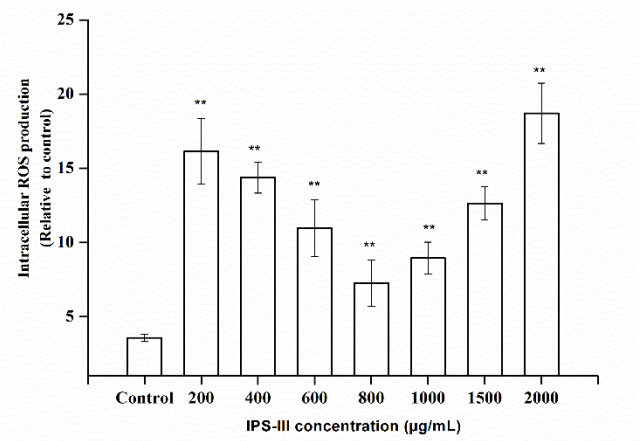

Fig. 11. The effect of IPS-III on ROS production in H_2O_2-induced HepG2 cells

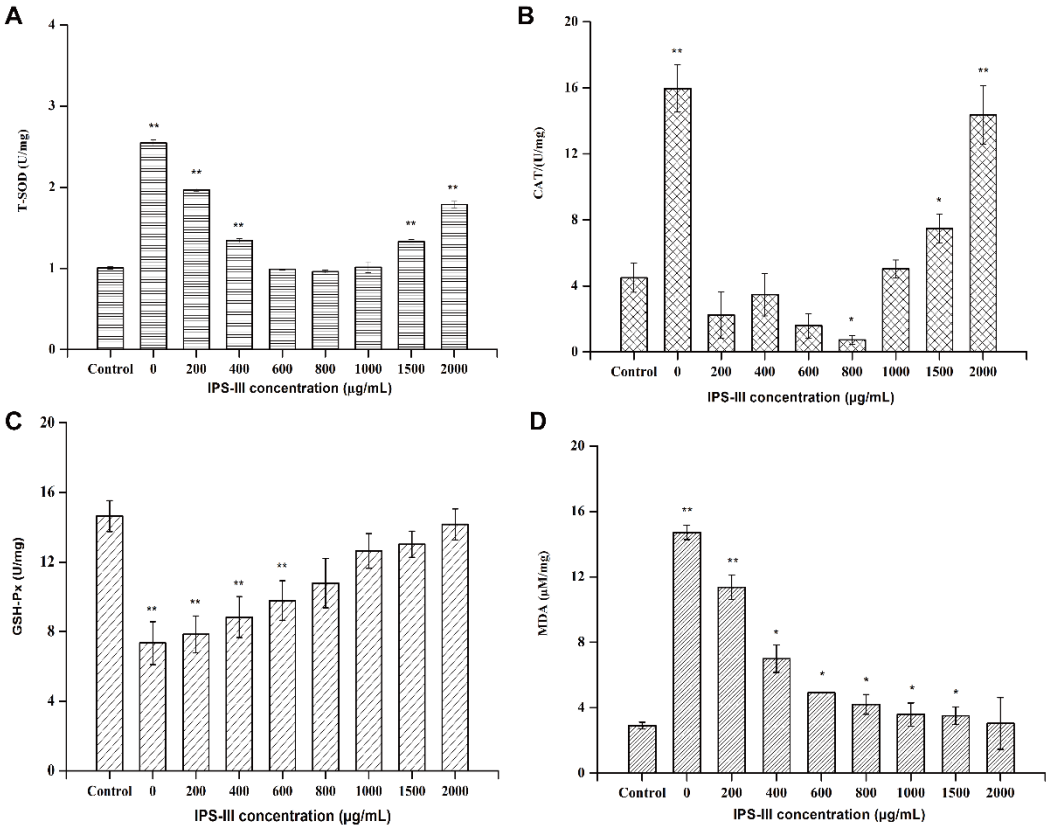

Fig. 12. The effect of IPS-III on T-SOD (A), CAT (B), GSH-Px (C) and MDA (D) in H_2O_2-induced HepG2 cells.

Author statement

Hui Kuang: Data curation, Writing-Original draft preparation; Yingchun Jiao: Visualization, Investigation; Wei Wang: Software, Validation; Fengju Wang: Visualization, Investigation; Qihe Chen: Conceptualization, Methodology, Writing- Reviewing and Editing, Supervision.

Highlights

1. The antioxidant activities of polysaccharides from *Agaricus bitorquis* (QuéL.) Sacc. Chaidam (ABSC) were investigated.
2. IPS was mainly composed of (1→6)-linked α-D-glucose.
3. IPS-III possesses a potent antioxidant ability both in *vitro* and inside HepG2 cells.
4. IPS-III protects HepG2 cells from H_2O_2-induced cytotoxicity by scavenging over-produced cellular ROS and inhibiting SOD, CAT and GSH depletion.